A New Necroptosis-Related lncRNA Signature Predicts the Prognosis and Tumor Immune Microenvironment of Breast Cancer Patients

Jinlai Zhao
Tianjin Medical University Cancer Institute and Hospital, National Clinical Research Center for Cancer
Haiyan Ma
Tianjin Medical University Cancer Institute and Hospital, National Clinical Research Center for Cancer
Ruigang Feng
Tianjin Medical University Cancer Institute and Hospital, National Clinical Research Center for Cancer
Dan Li
Tianjin Medical University Cancer Institute and Hospital, National Clinical Research Center for Cancer
Bowen Liu
Tianjin Medical University Cancer Institute and Hospital, National Clinical Research Center for Cancer
Yue Yu
Tianjin Medical University Cancer Institute and Hospital, National Clinical Research Center for Cancer
Xuchen Cao
Tianjin Medical University Cancer Institute and Hospital, National Clinical Research Center for Cancer
Xin Wang (xinwangse@126.com)
Tianjin Medical University Cancer Institute and Hospital, National Clinical Research Center for Cancer

Research Article

Keywords: necroptosis, lncRNAs, breast cancer, immune infiltration, drug therapy

Posted Date: May 3rd, 2022

DOI: https://doi.org/10.21203/rs.3.rs-1532933/v1

Abstract

Background: The issue of relationship between necroptosis and lncRNAs has been a controversial subject within cancer-related research. Currently, the exact role of necroptosis and lncRNAs exerted in breast cancer (BC) remains to be discovered. Therefore, the necroptosis-related lncRNAs in BC are explored in this study.

Methods: BC transcriptome data were obtained from the TCGA (The Cancer Genome Atlas) database to create synthetic matrices. Analysis approaches of univariate Cox regression and co-expression were combined to identify necroptosis-related prognostic lncRNAs. Then multivariate Cox regression and Lasso approaches were performed to acquire necroptosis-related lncRNAs, from which the predictive necroptosis-related lncRNA signature was constructed. Next, calibration curves, the time-dependent receiver operating characteristics (ROCs), ,and a nomogram were obtained, and the Kaplan-Meier analysis was performed to verify and evaluate the proposed model. Besides, the risk groups were analyzed with the Gene Set Enrichment Analyses (GSEA). Finally, these groups were studied by immune analysis to obtain the predicted half-maximal inhibitory concentration (IC50).

Results: A model was proposed based on 10 necroptosis-related lncRNAs, and the calibration plots accorded well with the predicted prognosis. For the 1-, 3-, and 5-year prognosis, the area under the ROC curve (AUC) values were 0.71, 0.729 and 0.707 respectively. GSEA identified that the functions of target genes located primarily in immunity, metabolism, as well as tumor occurrence and development. The remarkable differences in IC50 and gene expression between risk groups gave a significant insight for further systemic treatments. Besides, higher macrophage scores were found in the high-risk group, in which the patients were more sensitive to conventional chemotherapy drugs (such as AKT inhibitor VIII and saracatinib) and anti-CD80, TNF SF4, and CD276 immunotherapies.

Conclusion: The prognosis of BC patients can be independently predicted by the predictive signatures, which shines new insights on further exploration of how necroptosis-related lncRNAs exactly works in BC and clinical treatments of BC.

1. Introduction

Breast cancer (BC) ranks first in incidence and second only to lung cancer in mortality among common tumors in women, posing a great threat to female health. Recent years have witnessed great improvement in the survival of BC patients. However, the truth is that some patients still have a poor prognosis, and the incidence is increasing year by year[1]. Therefore, tools that are predictive to BC prognosis are essential to guide clinical diagnosis and treatment. As of today, BC prognosis in clinics relies heavily on evaluations of clinicopathological features, including age, lymph node metastasis, size of the tumor, and histological grades. According to PAM50, there are five molecular subtypes of BC, namely luminal A, luminal B, normal-like, basal-like, and Her2-enriched BC[2], and these five subtypes vary significantly in terms of their prognosis[3,4]. What's more, even BC patients of the same molecular subtype

and clinical representations show varied prognosis outcomes and responses to chemotherapy or immunotherapy[5], suggesting that the prognosis of BC and response of BC patients to treatment could be influenced by subtle factors.

Necroptosis is a form of programmed cell death that can be inhibited by necrostain-1 (Nec-1), which is a mode of death regulated by death signaling, and presents necrosis-like structural characteristics[6]. Specifically, necroptosis depends on several enzymes, namely the MLKL, RIPK1, and RIPK3[7], and is correlated to the pathogenesis of a variety of diseases as well as the pathogenesis of tumors. More particularly, tumor extravasation and migration could be promoted by necroptosis. One pathway of such promotion is associated with the mediation of expressed amyloid under which the tumor cells induce necroptosis in the endothelial cells via DR6 on the latter cells[8]. Besides, when genetically inactivated, RIPK3 or TNFR1 may alleviate the clinical symptoms of cancer and colitis, suggesting that necroptosis with active RIPK3 can promote the occurrence of chronic inflammation and colorectal cancer[9,10].

Literature has verified that long noncoding RNAs (lncRNAs) can function in cell proliferation, cell differentiation as well as the genetic regulation of gene expression[11]. More specifically, certain lncRNAs were found to release miRNAs that are capable to downregulate the expression of target mRNAs, making hepatocellular carcinoma cells undergo necroptosis. Besides, research has revealed that some lncRNAs can promote tumor inflammation and evasion of immune destruction[12]. Despite these findings, studies on necroptosis-related lncRNAs remain inadequate, especially for BC.

In this study, the necroptosis-related lncRNAs in BC were identified and clarified for their roles in prognosis and the tumor microenvironment (TME). To figure out the potential mechanisms, we, therefore, carried out gene enrichment analyses (KEGG and GO).

2. Materials And Methods

2.1 Identification of Necroptosis-Related lncRNAs

Several RNA transcriptome datasets (HTSeq—FPKM) and their relevant clinical information were obtained from The Cancer Genome Atlas (TCGA) database (https:// portal.gdc.cancer.gov/) to construct the synthetic data matrices of BC and normal breast tissues. The total number of normal and BC breast tissue samples obtained was 113 and 1109, respectively. Samples with a follow-up time < 30 days were excluded during screening. All the original data used in this study were downloaded from TCGA and complied with the TCGA publication guidelines (http://cancergenome.nih.gov/abouttcga/policies/publicationguidelines); therefore, ethics approval was not needed.

2.2 Screening of LncRNAs and Necroptosis-Related Genes

LncRNA data were derived from the RNA seq dataset. Log2 transformation was used to standardize the total RNA expression data. The list of all necroptosis-related genes was acquired from the KEGG

database (https://www.kegg.jp/entry/hsa04217), and the “limma” package was implemented to correlate necroptosis-related genes with lncRNAs. If an lncRNA demonstrated a correlation coefficient $|R^2|>0.3$ with $p < 0.001$, then it was considered a necroptosis-related lncRNA. LncRNA-mRNA correlations were calculated by the Pearson method and a correlation coefficient $|R^2|>0.3$ with $p < 0.01$ was adopted as an indicator of a correlation between a specific pair of lncRNA and mRNA. Finally, Cytoscape v3.7.2 was applied to visualize the lncRNA-mRNA co-expression networks.

2.3 Functional Enrichment Analysis of Necroptosis-Related Genes

If a differentially expressed gene (DEG) was to be considered necroptosis-related, it must satisfy two screening criteria: a |log 2-fold change (FC) > 1| and a false discovery rate (FDR) < 0.05. These two criteria were adopted in the subsequent GO and KEGG analyses in the “ggplot2” package (Fig. 1).

2.4 Identification of Prognostic Necroptosis-Related lncRNAs

In the beginning, a series of necroptosis-related lncRNAs that are associated with BC prognosis were identified via univariate Cox regression analysis. Subsequently, Lasso and multivariate Cox regression analyses were implemented to further identify necroptosis-related lncRNAs to construct the predictive signature for these lncRNAs with the following computational formula:

$$\text{risk score} = \sum_{i=1}^{n} * (\text{Coef}_i * x_i)$$

Where Coef stands for the coefficient, and x reflects how much the selected necroptosis-related lncRNAs have expressed. With this equation, a risk score could be obtained for each BC patient, and the patients may be assigned into either high-risk or low-risk groups based on their median risk scores[13,14]. The survival of the two groups was compared by a log-rank test.

2.5 Development of a Prognostic Model

The independent prognostic model was constructed with Cox regression, and patient survival was predicted with a nomogram. Model accuracy was evaluated with the concordance index (C-index), calibration curves, and receiver operating characteristic (ROC) curves. Finally, the multivariate Cox regression analysis integrated the demographic data to investigate whether the risk score is an independent indicator of BC prognosis.

2.6 Functional Analysis

The functional enrichment data of gene expressions were interpreted via gene set enrichment analysis (GSEA, http://www.broadinstitute.org/gsea/index.jsp)[15]. A prognostic value was assigned to the functional enrichment of each necroptosis-related lncRNA, and the top 5 necroptosis-related GO and KEGG pathways were visualized.

2.7 Clinical Investigations of the TME, Immune Checkpoints, and the Model

To help improve the immunotherapy of BC, Limma, GSVA, GSEABase, ggplot2, and ggpubr R packages were implemented to evaluate the different expressions of 47 immune checkpoint genes in 29 types of immune cells in the assigned risk groups[14]. IC50 differences were assessed by "PRRopheti" and other R packages in both risk groups for improvements in BC chemotherapy[16].

2.8 Statistical Analysis

All statistical analyses were performed using R software (Version 4.1.2). Wilcoxon test was implemented to analyze the expression of necroptosis-related DEGs in normal and BC tissue samples. In order to form a predictive signature, the correlations between overall survival (OS) and necroptosis-related lncRNAs were investigated by univariate Cox regression analysis, followed by screening for necroptosis-related lncRNAs with multivariate Cox analysis. The OS values of both risk groups were studied by the log-rank test and the Kaplan-Meier method. The ROC curves and AUC values were obtained by applying the “survivalROC” package.. All statistical tests were bilateral, and $p < 0.05$ was considered statistically significant.

3. Results

3.1 Identification of Prognostic Necroptosis-Related LncRNAs

14,142 lncRNAs were identified from TCGA-COAD, in which 1098 were necroptosis-related. More specifically, associations with BC prognosis were found in 56 of these 1098 lncRNAs. Lasso Cox regression analysis revealed 16 necroptosis-related lncRNAs that are connected to BC prognosis (Fig. 2), while multivariate Cox regression analysis revealed only 10. Specifically, AL606834.2, SEMA3B-AS1, AL731571.1, OTUD6B-AS1, BAIAP2-DT, Z68871.1, EGOT, AL136531.1, LINC01871, and AL122010.1 were combined to build a predictive signature (Table 1). The overall risk score was calculated by the following equation (in which the names of the lncRNAs represent their corresponding expression levels): risk score = (-0.216 × AL606834.2) +(-0.074 × SEMA3B-AS1) +(-0.318 × AL731571.1) +(0.049×OTUD6B-AS1) + (-0.051×BAIAP2-DT) +(0.448 × Z68871.1) +(-0.091 × EGOT) +(-0.380 × AL136531.1) +(-0.253 × LINC01871) +(-0.244 × AL122010.1).

The Cytoscape software and R software packages of ggalluvial and ggplot were implemented to visualize the lncRNAs. The co-expression network and linear correlation plots contained 39 pairs lncRNA-mRNA (Fig. 3 and Fig. 4, $|R^2|>0.3$, $p < 0.001$). 10 lncRNA-mRNA linear correlation plots were included in our study (Fig. 3). From the Sankey diagram, in terms of the nature of the prognostic factors, two lncRNAs (OTUD6B-AS1 and Z68871.1) were harmful, and the remaining ones (AL606834.2, SEMA3B-AS1, AL731571.1, BAIAP2-DT, EGOT, AL136531.1, LINC01871, and AL122010.1) were favorable (Fig. 4).

Table 1
Results of multivariate Cox analysis of the lncRNAs based on TCGA COAD data.

LncRNA	Coefficient	HR	95%CI of HR
AL606834.2	-0.216	0.806	0.610–1.065
SEMA3B-AS1	-0.074	0.929	0.870–0.992
AL731571.1	-0.318	0.727	0.499–1.060
OTUD6B-AS1	0.049	1.050	0.989–1.115
BAIAP2-DT	-0.051	0.950	0.900-1.004
Z68871.1	0.448	1.565	1.095–2.236
EGOT	-0.091	0.913	0.812–1.026
AL136531.1	-0.380	0.684	0.458–1.020
LINC01871	-0.253	0.776	0.676–0.892
AL122010.1	-0.244	0.783	0.650–0.994

3.2 The Prognostic Effect of the Constructed Signature

Results showed a significant correlation between the established risk score and the OS of BC patients, with the low-risk group exhibiting longer OS ($p < 0.001$, log-rank test) (Fig. 5). Cox regression results suggested that the risk scores have marked prognostic effects for BC patients (Fig. 6).

3.3 Clinical Significance of the Proposed LncRNA Signature

The univariate Cox regression analysis results suggested a significant correlation between age, disease stages (T, N & M), the risk scores and the OS of BC patients (Fig. 7(a)). Furthermore, the multivariate Cox regression analysis revealed that for BC patients, risk scores and age were two independent predictors of OS (Fig. 7(b) and Table 2). Besides, the risk score demonstrated an AUC of 0.719, which was more favored compared to clinicopathological variables when predicting BC prognosis (Fig. 7(c)). The AUCs of 1, 3, and 5-year survival curves were 0.71, 0.729 and 0.707, respectively, suggesting that the predictive performance was satisfactory (Fig. 7(d)). Moreover, the two risk groups varied significantly in their clinicopathological variables among all disease stages studied ($p < 0.05$) (Fig. 7(e) and Table 3).

Table 2
Risk scores and clinical characteristics of BC (analyzed with multivariate Cox regression).

Variable	B	SE	Z	HR	HR95L	HR95H	Pvalue
Age	0.032	0.008	4.224	1.032	1.017	1.048	< 0.001
Gender	-0.277	1.011	-0.274	0.758	0.105	5.499	0.784
Stage	0.430	0.267	1.614	1.538	0.912	2.593	0.107
T	-0.040	0.155	-0.256	0.961	0.709	1.302	0.780
M	0.764	0.437	1.748	2.146	0.912	5.051	0.080
N	0.170	0.154	1.104	1.185	0.877	1.601	0.270
Risk score	0.449	0.060	7.550	1.567	1.395	1.761	< 0.001

In order to produce more accurate predictions of BC prognosis, a nomogram was constructed, in which the risk score and clinicopathological variables were included to predict the 1, 3, and 5-year BC prognosis (Fig. 8(a)). The calibration curves were highly consistent with the actual and predicted OS rates at these aforementioned time periods (Figs. 8(b-d)).

Table 3
Clinical effects of the risk score signature (as identified by the TCGA-COAD data).

Risk score					
clinical	n	Mean	SD	t	P
Age					
> 65	222	1.601	1.181	1.92	0.056
≤ 65	642	1.429	1.06		
Gender					
Female	835	1.475	1.097	0.49	0.634
Male	11	1.347	0.855		
Stage					
I-II	661	1.386	1.039	-3.92	< 0.05
III-IV	203	1.757	1.217		
T					
T1-2	739	1.437	1.056	-2.07	0.04
T3-4	125	1.687	1.28		
M					
M0	848	1.468	1.098	-1.40	0.181
M1	16	1.774	0.864		
N					
N0	422	1.388	1.052	-2.24	0.025
N1-3	442	1.555	1.128		

3.4 Functional Analysis.

178 KEGG pathways and 5375 GO terms were obtained for the functional analysis. The GO terms indicated that the necroptosis-related lncRNAs were concentrated in signal transduction, metabolism, and immune-related regulations (Fig. 9(a)). On the other hand, KEGG pathways of the lncRNAs were focused in malignant tumor formation, autoimmune diseases, metabolic diseases, metabolism, signal transduction, etc. (Fig. 9(b)). Furthermore, the gene sets were also revealed to be significantly correlated with vital pathways of tumorigenesis and cancer progression. For example, WNT and VEGF signaling

pathways, as well as the tumor necrosis factor receptor were closely related to cancer invasion and metastasis.

3.6 Immune Cell Infiltration

In this section, the enrichment scores of GSEA were quantified for various immune cell subgroups to reveal deeper about the correlations between immune cells and risk scores. All the cells showing significant expression differences between the risk groups are displayed in Fig. 10.. Specifically, only macrophages exhibited a higher score in the high-risk group, suggesting that these cells are more functionally active in this group.

3.7 Correlations Between the BC Therapy and the Predictive Signature

CD80, TNFSF4, and CD276 expressions were remarkably higher in the high-risk group, suggesting that patients with a high-risk predictive signature may exhibit the potential to respond to anti-CD80, TNFSF4, or CD276 immunotherapies (Fig. 11(a)). Besides, the high-risk group demonstrated lower IC50 values of AKT inhibitor VIII, Saracatinib, Bicalutamide, Imatinib, Lapatinib, Linsitinib, and Pazopanib (Figs. 11(b-h)) but a higher IC50 value of Methotrexate (Fig. 11(i)) than the low-risk group, which provided more insights on developing new individualized treatment schemes for BC patients.

4. Discussion

BC is the predominant malignant tumor that endangers female physical and mental health. BC incidence has been rising year by year, and the tendency for rejuvenation is obvious, presenting an urgent need for an accurate tool to predict BC prognosis for improvements in clinical diagnosis and treatment. Necroptosis occurs under the mediation of death receptors and their ligands when the apoptotic pathways are inhibited[17]. In cancer, necroptosis plays complex roles, especially in cancer development and progression[18]. As of today, no previous reports have attempted to predict BC prognosis by constructing predictive signatures based on necroptosis-related lncRNAs.

In this study, a co-expression network of necroptosis-related genes and lncRNA was implemented to screen the necroptosis-related lncRNAs. Furthermore, Cox and Lasso regression analyses were implemented to reveal 10 prognostic necroptosis-related lncRNAs, namely AL606834.2, SEMA3B-AS1, AL731571.1, BAIAP2-DT, EGOT, AL136531.1, LINC01871, AL122010.1, OTUD6B-AS1, and Z68871.1. These lncRNAs may serve as the potential therapeutic targets and prognostic molecular markers for BC patients. Besides, several mRNAs (e.g. BCL2, BIRC3, CFLAR, CHMP2A, CHMP4A, CHMP4C, JMJD7a, and TRPM7) were also found to significantly co-express with these lncRNAs.

Three necroptosis-related lncRNAs (SEMA3B-AS1, EGOT, OTUD6B-AS1) were revealed to be cancer-associated. Specifically, an upregulation of SEMA3B-AS1 was found in hepatocellular carcinoma (HCC) and the overexpression of the lncRNA may promote PTEN expression, which could in turn inhibit the

proliferation of hepatocellular carcinoma cells. Besides, SEMA3B-AS1 is also a prognostic marker for HCC[19]. Firstly, previous research has shown that SEMA3B, miR-6872-5p, and SEMA3B-AS1 may impose tumor-suppressive effects in the tumorigenesis of gastric cardia adenocarcinoma. Moreover, these molecules may also be used as potential markers in predicting the survival and prognosis of gastric cardia adenocarcinoma patients[20]. Secondly, EGOT upregulation is marked in gastric cancer (GC), and such upregulation is related to the TNM stages and lymphatic metastasis. In addition, siRNA-mediated EGOT knockdown could provide a marked inhibition on GC cell proliferation and arrest cell cycles in the G1 phase. As an oncogene in GC, EGOT could be adopted as a convincing biomarker for GC diagnosis and prognosis[21]. Thirdly, OTUD6B-AS1 was found to be downregulated in thyroid carcinoma (TC) tissues, and its expression is correlated with size of the tumor size, clinical stages, and the lymphatic metastasis of TC. Besides, OTUD6B-AS1 overexpression demonstrated a significant and negative correlation with the viability as well as the migration and invasion capabilities of TC cells[22].

The three necroptosis-related lncRNAs (BAIAP2-DT, LINC01871, Z68871.1) can be used as markers for the prognosis of BC, but the pathogenesis of BC has not yet been studied in depth[23]. As for the other 4 lncRNAs (AL606834.2, AL731571.1, AL136531.1, AL122010.1), no previous studies have been published about their prognostic roles in cancer.

In this study, 10 necroptosis-related lncRNAs were used to construct a signature model that can predict BC prognosis with satisfactory prediction performance. Specifically, compared to the predicted high-risk group, the predicted low-risk group exhibited longer OS, which had been revealed in previous studies. The AUC values corresponding to 1, 3, and 5-year survival were 0.71, 0.729 and 0.707, respectively, indicating some potential in the constructed risk score signature to predict survival. Besides, according to the results of univariate and multivariate Cox analyses, the constructed signature is an independent prognostic indicator. C-index results, ROC curves, and calibration curves suggested that the model proposed in this study exhibited good precision and accuracy, demonstrating the model's potential as a predictive tool for BC patients.

Functional enrichment analysis found that the identified necroptosis-related prognostic lncRNAs were enriched in signal transduction, metabolism, immune-related regulations as well as the formation of malignant tumors. Furthermore, the gene sets were revealed to be correlated to tumorigenesis and cancer progression, which has provided more information about the mechanisms of the effects of necroptosis-related lncRNAs. Previous studies have suggested that necroptosis signaling may involve in the proliferation and migration of BC cells. Specifically, the key components of necroptosis signaling were identified to correlate significantly with the pathological and clinical parameters of BC, and such correlations were present regardless of TNM stages and pathological subtypes; therefore, necroptosis activation could be a common phenomenon along with BC development. In addition, necroptosis activation was well correlated with TNFα expression, and TNFα is a key pro-inflammatory factor that recruits immune cells to tumors. In a word, necroptosis signaling pathways are endogenous protective

pathways in human systems, and these pathways are activated to counter tumor malignancy, representing a potential target for BC therapy[24].

Subsequent GSEA results showed that the high-risk group exhibited higher macrophage scores. Previous studies have revealed that tumor-associated macrophages (TAMs) can promote tumorigenesis in the BC microenvironment. In BC models, preclinical TAMs were found to possibly stimulate the tumor cell growth,, invasion, and metastasis of BC while inducing resistance against multiple treatments[25].

Besides, this study also showed that high-risk patients as identified by the proposed model are possibly more sensitive to anti-CD80, TNF SF4, or CD276 immunotherapies and conventional chemotherapy drugs (including AKT inhibitor VIII, Saracatinib, Bicalutamide, Imatinib, Lapatinib, Linsitinib, and Pazopanib) while being more resistant to methotrexate, suggesting that these BC patients can benefit from the individualized and precise combination of immunotherapies and chemotherapies.

However, this research still exhibit certain limitations. First, data from other databases are needed to perform external validation on our predictive signature for its applicability. Second, the action mechanisms of the necroptosis-related lncRNAs in BC still need more investigations.

5. Conclusions

In summary, the proposed necroptosis-related lncRNA signature is capable to predict BC prognosis as an independent indicator and provide insights about the possible action mechanisms of these lncRNAs in BC and the patients' responses to clinical treatment, but further experimental verification is still needed.

Abbreviations

LASSO	Least Absolute Shrinkage and Selection Operator
K-M	Kaplan-Meier
IC50	The half-maximal inhibitory concentration
HR	Hazard ratio
Nec-1	Necrostain-1
RIPK1	Receptor-interacting serine/threonine protein kinase 1
RIPK3	Receptor-interacting serine/threonine protein kinase 3
miRNA	MicroRNA
TME	Tumor microenvironment
FDR	False discovery rate
FC	Fold change
BP	Biological process
MF	Molecular function
iDCs	Immature dendritic cells
pDCs	Plasmacytoid dendritic cells
Tfh	T follicular helper
Th1	T helper type 1
TIL	Tumor infiltrating lymphocyte
Treg	T regulatory cell
ns	Non-significant

Declarations

Ethical Approval and Consent to participate

Not applicable

Consent for publication

Not applicable

Availability of data and materials

All data generated or analyzed during this study are included in this published article and its supplementary information files.

Competing interests

The authors declare that there are no conflicts of interest regarding the publication of this study.

Funding

This study was supported by the grants from National Natural Science Foundation of China (No. 8217103088).

Authors' contributions

WX designed the study; ZJL performed the statistical analysis and drafted the paper; MHY and YY reviewed and revised the paper. FRG,LD,LBW and CXC performed some data analyses.All authors read and approved the final manuscript.

Acknowledgments

Thanks to all the staff involved in setting up the TCGA database.

References

1. Miller, K. D.*et al.* Cancer treatment and survivorship statistics, 2016. *CA: a cancer journal for clinicians* **66**, 271-289, doi:10.3322/caac.21349 (2016).
2. Pu, M.*et al.* Research-based PAM50 signature and long-term breast cancer survival. *Breast cancer research and treatment* **179**, 197-206, doi:10.1007/s10549-019-05446-y (2020).
3. Kumar, M.*et al.* BRCA1 Promoter Methylation and Expression - Associations with ER+, PR+ and HER2+ Subtypes of Breast Carcinoma. *Asian Pacific journal of cancer prevention : APJCP* **18**, 3293-3299, doi:10.22034/apjcp.2017.18.12.3293 (2017).
4. Meisel, J.*et al.* Evaluation of Prognosis in Hormone Receptor-Positive/HER2-Negative and Lymph Node-Negative Breast Cancer With Low Oncotype DX Recurrence Score. *Clinical breast cancer* **18**, 347-352, doi:10.1016/j.clbc.2017.12.006 (2018).
5. Tekpli, X.*et al.* An independent poor-prognosis subtype of breast cancer defined by a distinct tumor immune microenvironment. *Nature communications* **10**, 5499, doi:10.1038/s41467-019-13329-5 (2019).
6. Galluzzi, L.*et al.* Molecular definitions of cell death subroutines: recommendations of the Nomenclature Committee on Cell Death 2012. *Cell death and differentiation* **19**, 107-120, doi:10.1038/cdd.2011.96 (2012).
7. Galluzzi, L.*et al.* Molecular mechanisms of cell death: recommendations of the Nomenclature Committee on Cell Death 2018. *Cell death and differentiation* **25**, 486-541, doi:10.1038/s41418-017-

0012-4 (2018).

8. Strilic, B.*et al.* Tumour-cell-induced endothelial cell necroptosis via death receptor 6 promotes metastasis. *Nature* **536**, 215-218, doi:10.1038/nature19076 (2016).
9. Shi, J.*et al.* Loss of periodontal ligament fibroblasts by RIPK3-MLKL-mediated necroptosis in the progress of chronic periodontitis. *Scientific reports* **9**, 2902, doi:10.1038/s41598-019-39721-1 (2019).
10. Tortola, L.*et al.* The Tumor Suppressor Hace1 Is a Critical Regulator of TNFR1-Mediated Cell Fate. *Cell reports* **15**, 1481-1492, doi:10.1016/j.celrep.2016.04.032 (2016).
11. Mercer, T. R., Dinger, M. E. & Mattick, J. S. Long non-coding RNAs: insights into functions. *Nature reviews. Genetics* **10**, 155-159, doi:10.1038/nrg2521 (2009).
12. Dragomir, M. P., Kopetz, S., Ajani, J. A. & Calin, G. A. Non-coding RNAs in GI cancers: from cancer hallmarks to clinical utility. *Gut* **69**, 748-763, doi:10.1136/gutjnl-2019-318279 (2020).
13. T. Meng, R. Huang, Z. Zeng et al., "Identification of prognostic and metastatic alternative splicing signatures in kidney renal clear cell carcinoma," *Frontiers in Bioengineering and Biotechnology*, vol. 7, p. 270, 2019.
14. W. Hong, L. Liang, Y. Gu et al., "Immune-related lncRNA to construct novel signature and predict the immune landscape of human hepatocellular carcinoma," *Molecular :erapy - Nucleic Acids*, vol. 22, pp. 937–947, 2020.
15. Subramanian, A., Tamayo., P., Mootha, V. K., Mukherjee, S., Ebert, B. L., Gillette, M. A., et al. Gene Set Enrichment Analysis: A Knowledge-Based Approach for Interpreting Genome-Wide Expression Profiles. *Proc. Natl. Acad*. Sci. 102 (43), 15545–15550,2005.
16. P. Geeleher, N. J. Cox, and R. Huang, "Clinical drug response can be predicted using baseline gene expression levels and in vitro drug sensitivity in cell lines," *Genome Biology*, vol. 15, no. 3, p. R47, 2014.
17. Degterev, A.*et al.* Chemical inhibitor of nonapoptotic cell death with therapeutic potential for ischemic brain injury. *Nature chemical biology* **1**, 112-119, doi:10.1038/nchembio711 (2005).
18. Shi, s., Qin, X., Wang, H. & Cai, Z. in *Progress in Biochemistry and Biophysics* Vol. 47□7□ 561-573 (2020).
19. Kalantari, P.*et al.* miR-718 represses proinflammatory cytokine production through targeting phosphatase and tensin homolog (PTEN). *The Journal of biological chemistry* **292**, 5634-5644, doi:10.1074/jbc.M116.749325 (2017).
20. Guo, W.*et al.* MiR-6872 host gene SEMA3B and its antisense lncRNA SEMA3B-AS1 function synergistically to suppress gastric cardia adenocarcinoma progression. *Gastric cancer : official journal of the International Gastric Cancer Association and the Japanese Gastric Cancer Association* **22**, 705-722, doi:10.1007/s10120-019-00924-0 (2019).
21. Peng, W., Wu, J., Fan, H., Lu, J. & Feng, J. LncRNA EGOT Promotes Tumorigenesis Via Hedgehog Pathway in Gastric Cancer. *Pathology oncology research : POR* **25**, 883-887, doi:10.1007/s12253-017-0367-3 (2019).

22. Wang, Z.*et al.* OTUD6B-AS1 Inhibits Viability, Migration, and Invasion of Thyroid Carcinoma by Targeting miR-183-5p and miR-21. *Frontiers in endocrinology* **11**, 136, doi:10.3389/fendo.2020.00136 (2020).
23. Li, X., Jin, F. & Li, Y. A novel autophagy-related lncRNA prognostic risk model for breast cancer. *Journal of cellular and molecular medicine* **25**, 4-14, doi:10.1111/jcmm.15980 (2021).
24. Shen, F.*et al.* Pharmacological Inhibition of Necroptosis Promotes Human Breast Cancer Cell Proliferation and Metastasis. *OncoTargets and therapy* **13**, 3165-3176, doi:10.2147/ott.S246899 (2020).
25. Qiu, S. Q.*et al.* Tumor-associated macrophages in breast cancer: Innocent bystander or important player? *Cancer treatment reviews* **70**, 178-189, doi:10.1016/j.ctrv.2018.08.010 (2018).

Figures

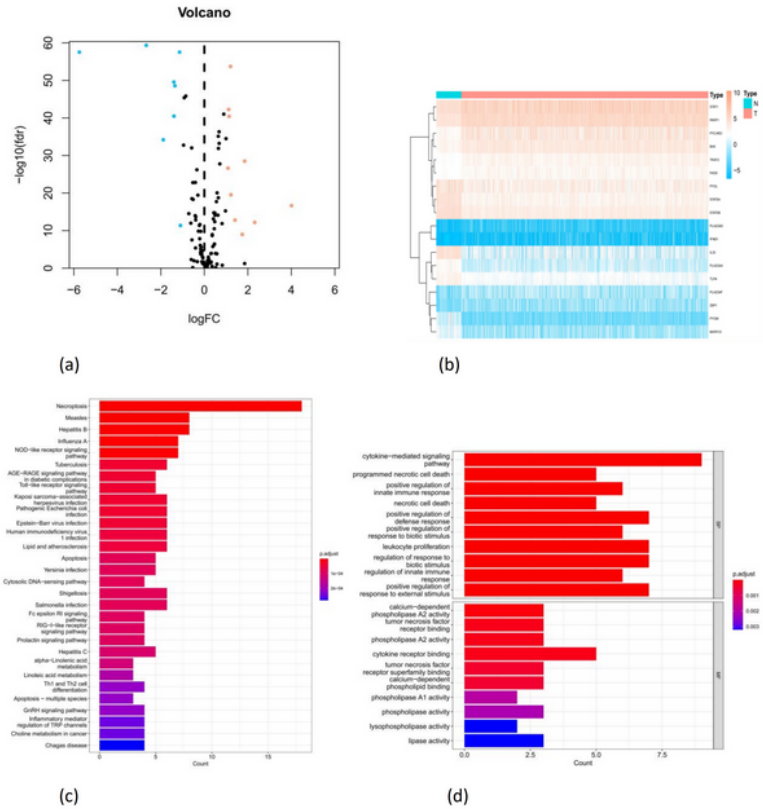

Figure 1

KEGG and GO analyses of necroptosis-related DEGs in BC and normal tissue samples. (a)Volcano plot of 18 necroptosis-related genes in BC. Blue and red dots represent down-regulated and up-regulated genes, respectively. (b) The expression levels of 18 necroptosis-related genes in BC and normal tissues. (c) KEGG analysis of necroptosis-related DEGs. (d) GO analysis of necroptosis-related DEGs. fdr: false discovery rate; MF: molecular function; FC: fold change; BP: biological process.

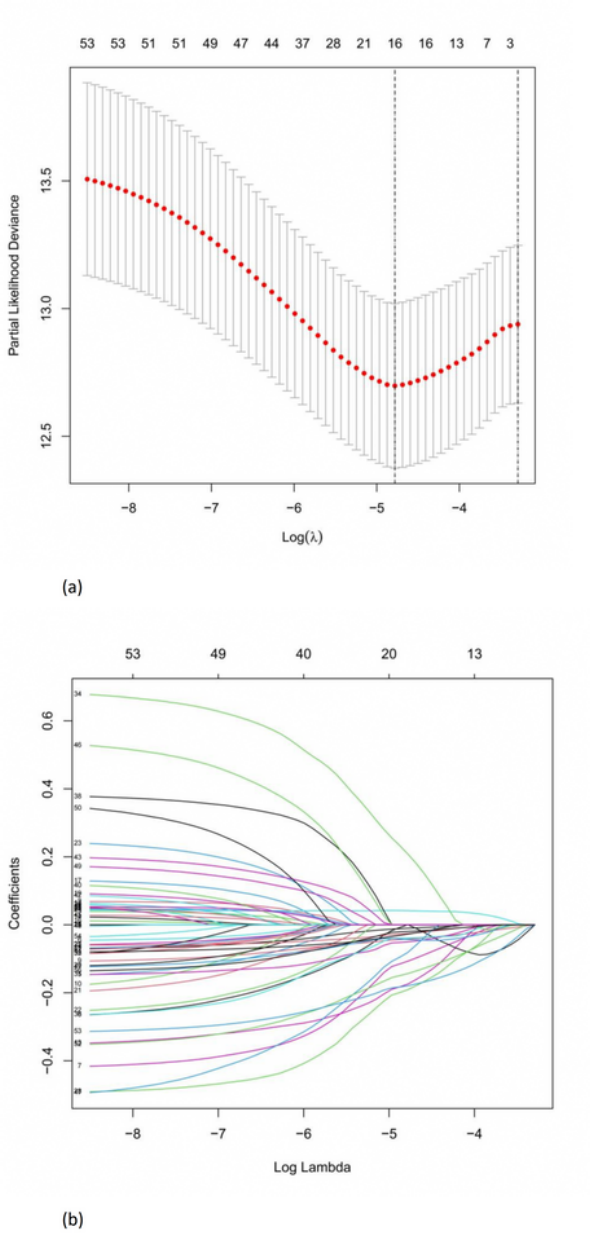

Figure 2

Lasso-based selection of necroptosis-related lncRNAs. (a) Lasso coefficients of the 16 necroptosis-related lncRNAs in BC, where the optimal log (lambda) value is marked by vertical dashed lines. (b) Lasso coefficient profiles.

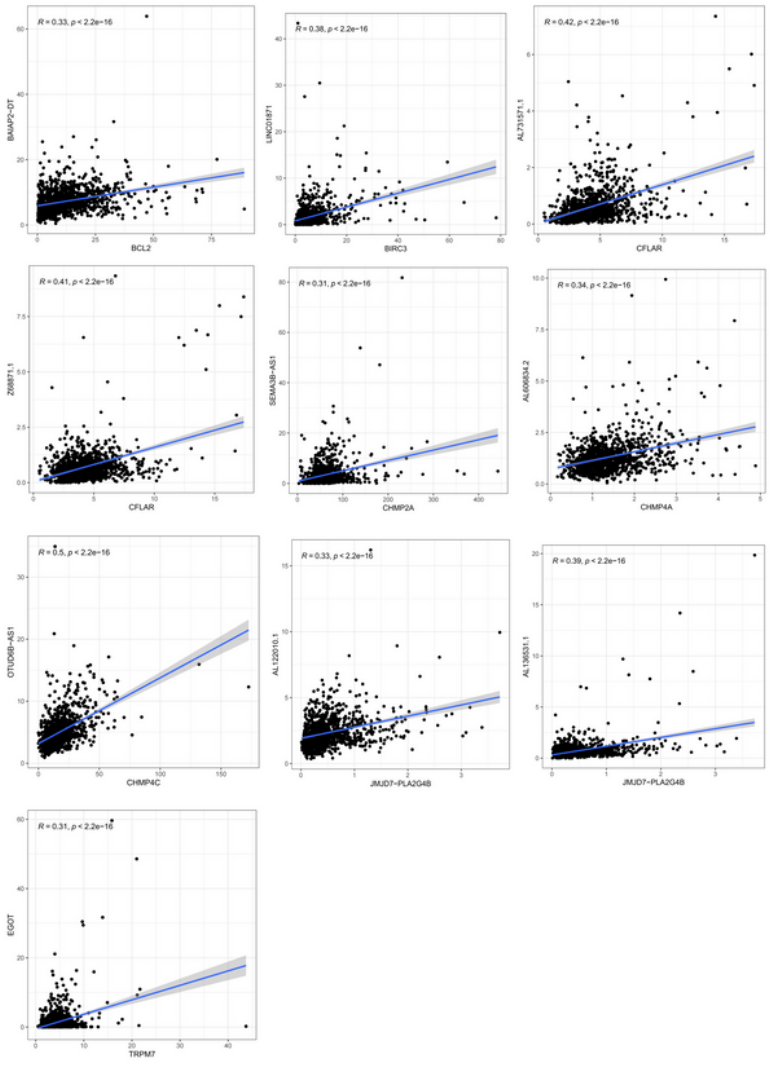

Figure 3

Linear correlation plot of necrosis-associated lncRNAs and mRNAs.

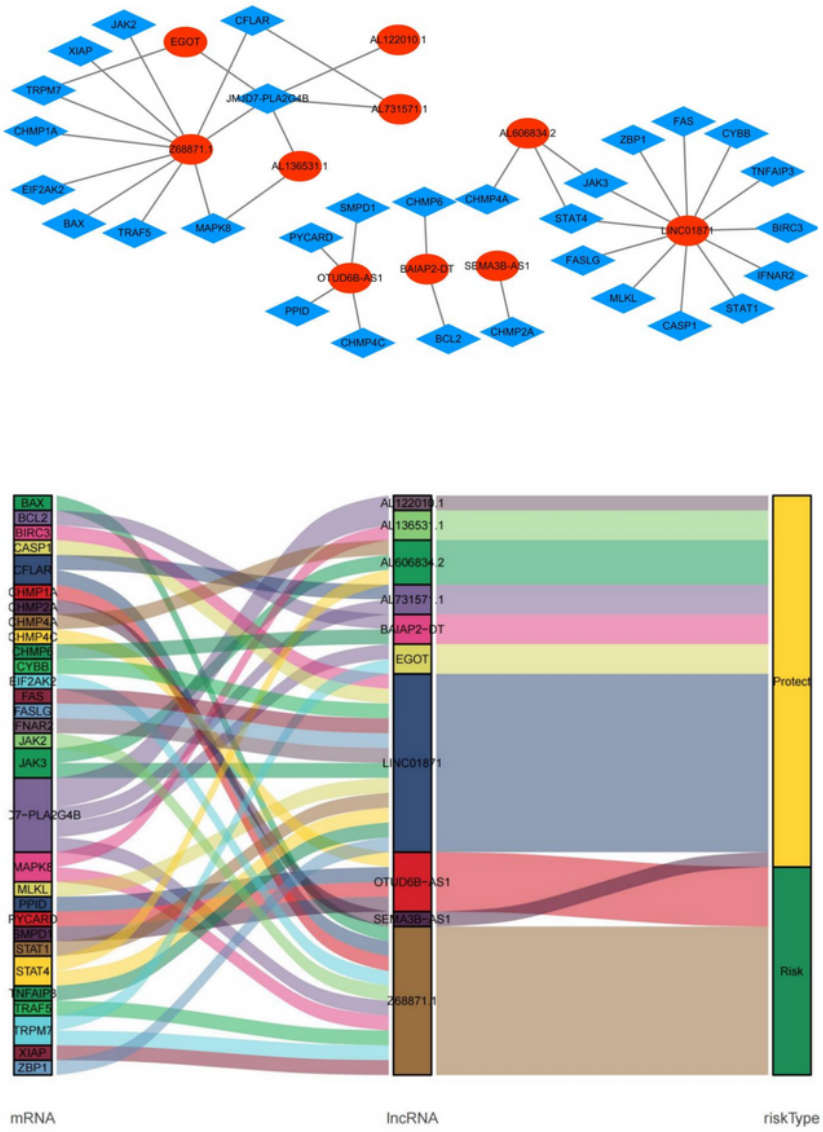

Figure 4

The Sankey diagram and co-expression network of necroptosis- and prognosis-related lncRNAs.(a) The co-expression network between the necroptosis-related genes (sky-blue round nodes) and prognostic lncRNAs (red diamond nodes) in BC. Network visualized by Cytoscape v3.7.2. (b) The Sankey diagram.

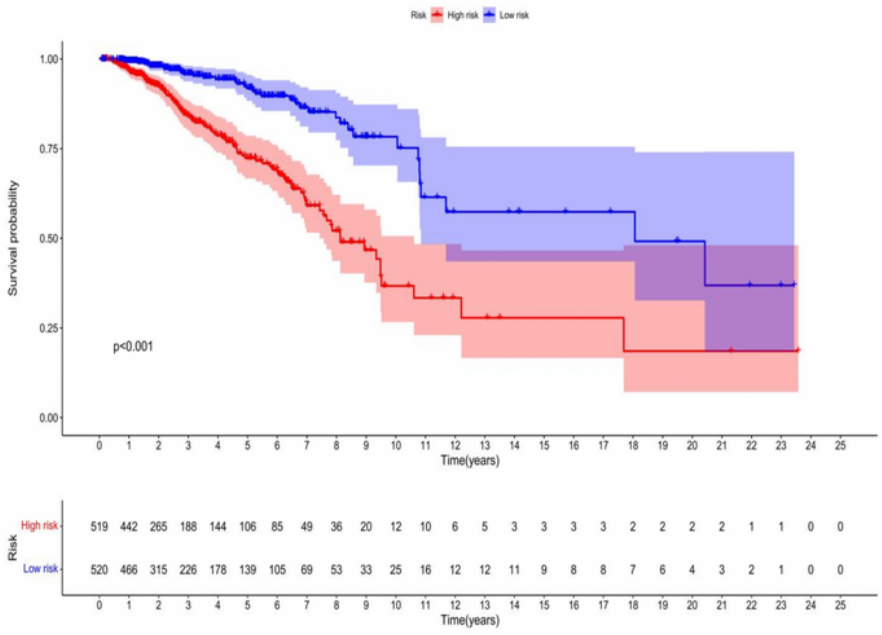

Figure 5

The KM survival curves of two risk groups based on 10 necroptosis-related lncRNAs.

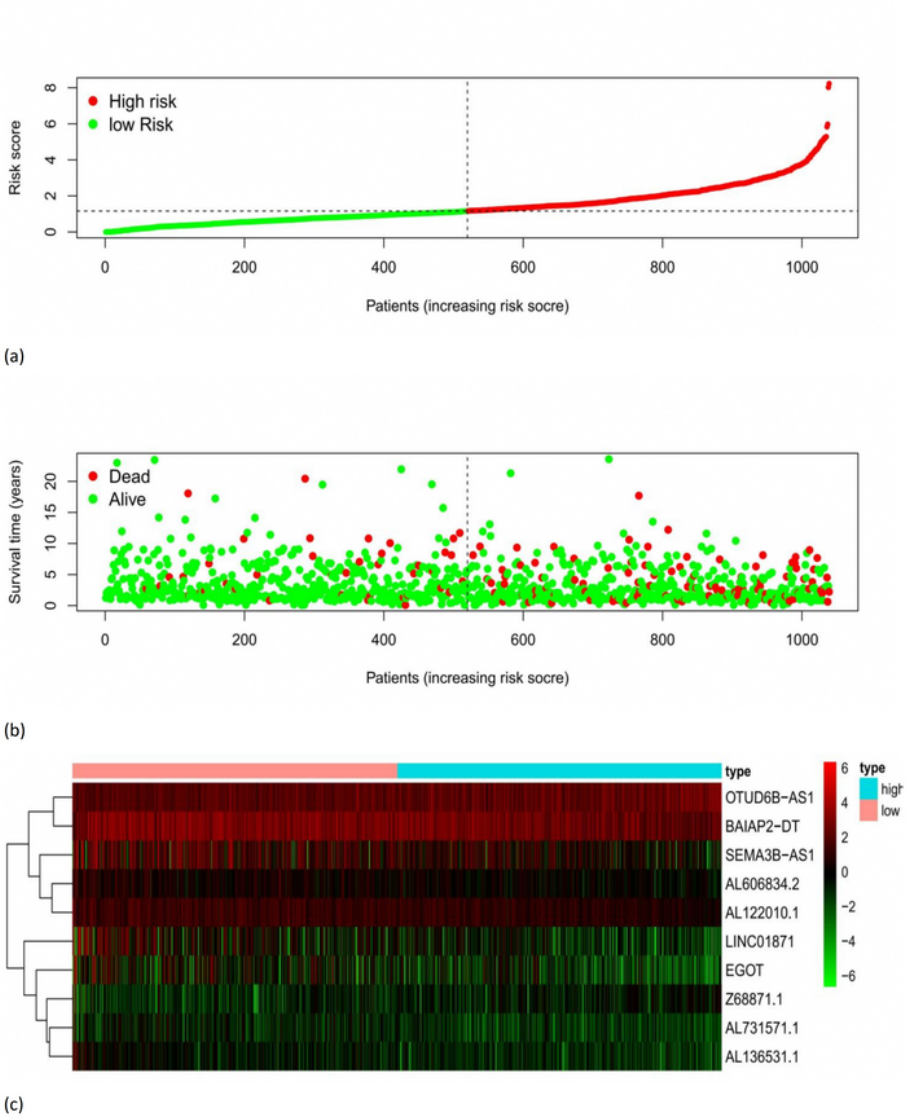

Figure 6

Necroptosis-related lncRNA signatures for BC patients. (a) The risk scores of the two risk groups. (b) The patients' survival time. (c) Heat map of the expression of the ten lncRNAs. As the color shifts red, the expression level becomes higher.

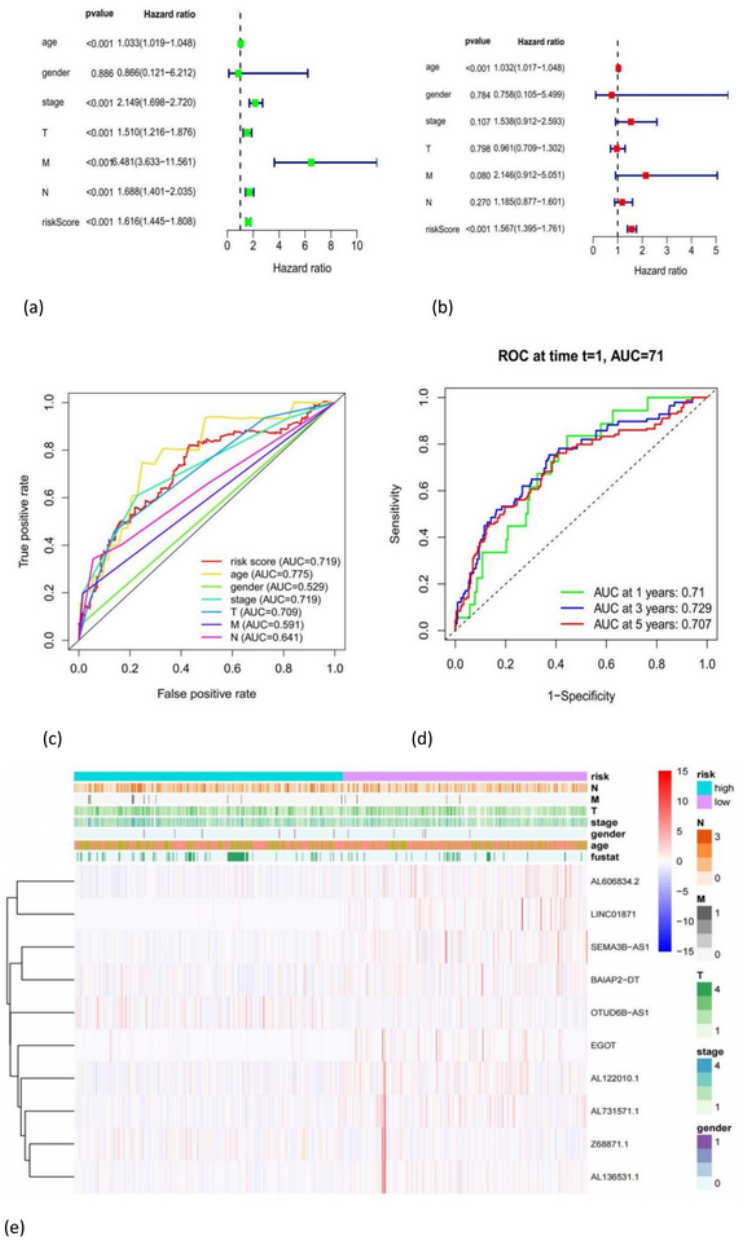

Figure 7

The correlation between BC prognosis and the proposed predictive signature . (a) The Forest plot for univariate Cox regression analysis. (b) The Forest plot for multivariate Cox regression analysis. (c) The ROC curve of the clinicopathological variables and the risk scores. (d) ROC curves and corresponding AUCs at 1, 3 and 5-year survival with the predictive signature. (e) The distribution heat map of the clinicopathological variables and ten prognostic lncRNAs in the two risk groups.

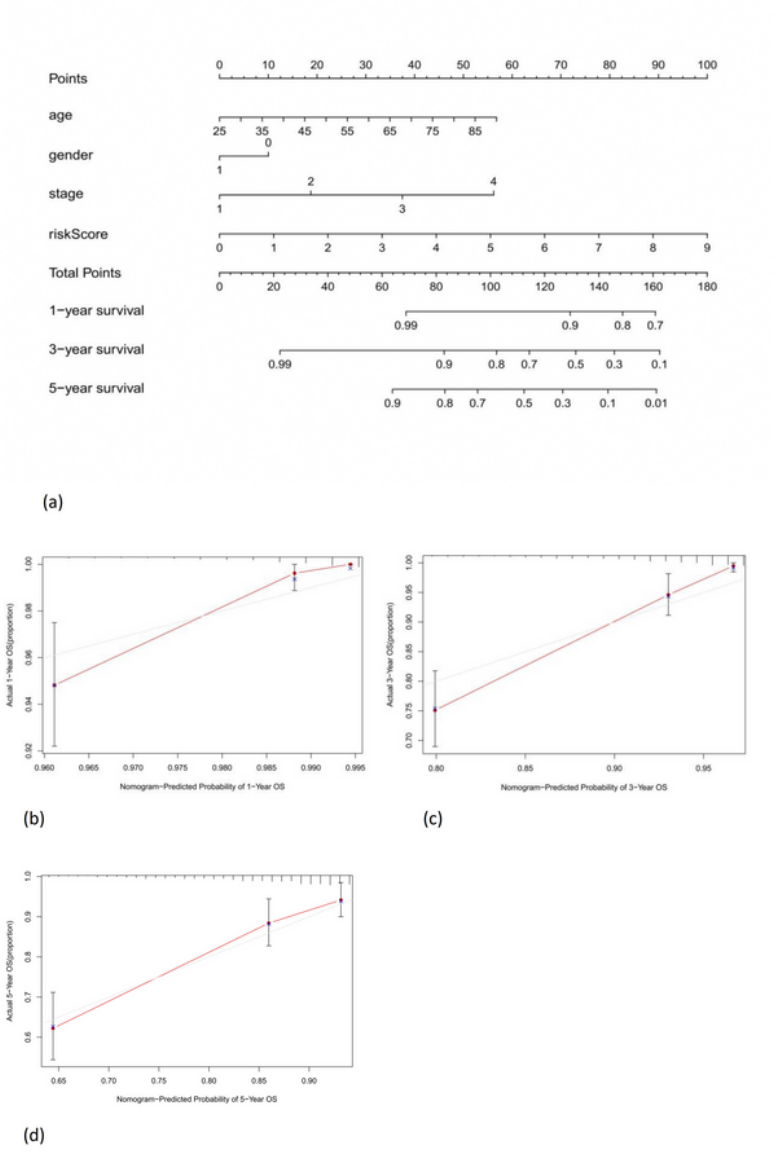

Figure 8

Nomogram construction and verification. (a) A nomogram combining risk scores and clinicopathological variables. (b-d) Calibration curves between the actual and predicted OS rates at 1, 3 and 5 years.

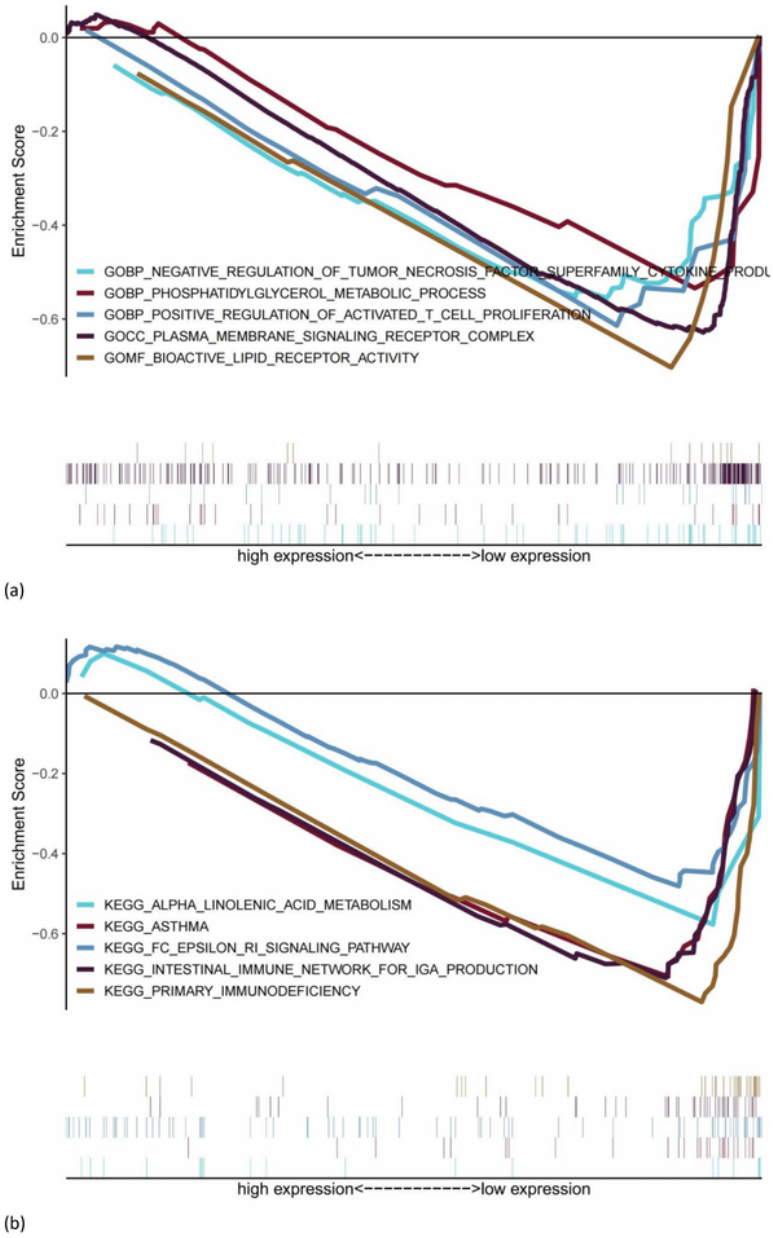

Figure 9

Functional analysis results for necroptosis-related lncRNAs. (a) GO; (b) KEGG.

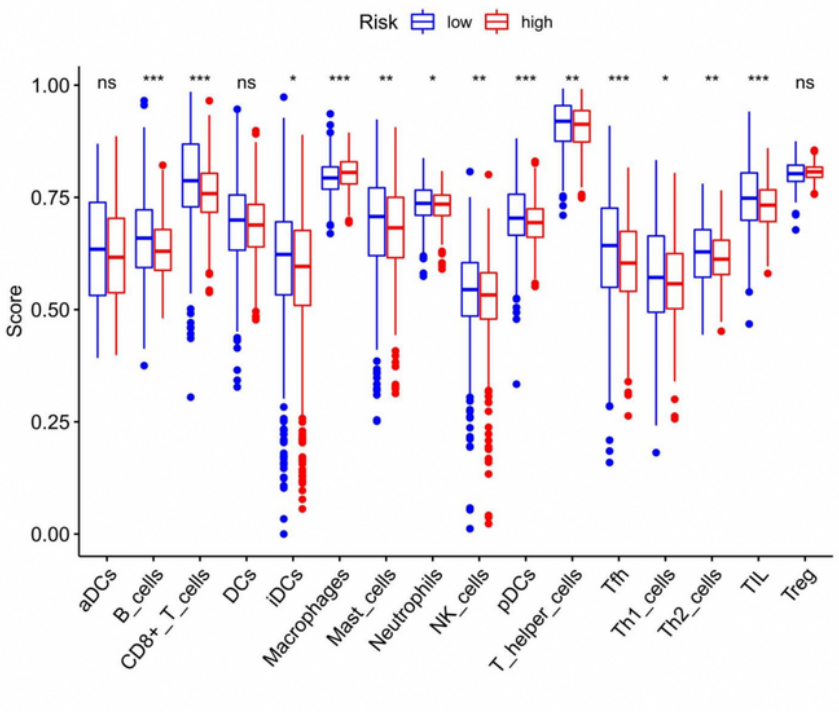

Figure 10

The scores of immune infiltrating cells in the two risk groups.

The GSEA algorithm was used to calculate the infiltration of the 16 immune cells in the two risk groups. * p<0.05; ** p<0.01; *** p<0.001; ns, non-significant.

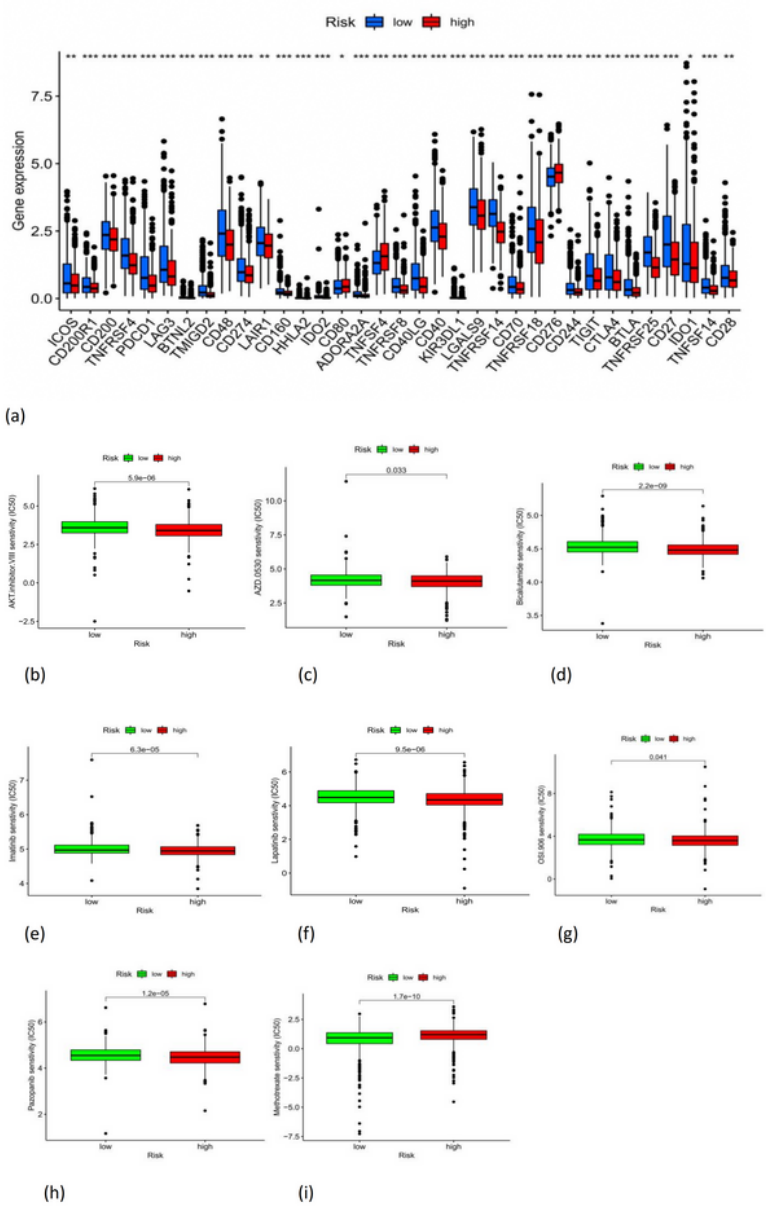

Figure 11

Sensitivity to treatment drugs in both risk groups.(a) CD80, TNF SF4, and CD276 expressions in the two risk groups. (b) IC50 of AKT inhibitor VIII in the two risk groups. (c) IC50 of AZD0530 (Saracatinib) in the two risk groups. (d) IC50 of Bicalutamide in the two risk groups. (e) IC50 of Imatinib in the two risk groups. (f) IC50 of Lapatinib in the two risk groups. (g) IC50 of OSI.906 (Linsitinib) in the two risk groups. (h) IC50 of Pazopanib in the two risk groups, (i) IC50 of methotrexate in the two risk groups.